Foreground Modeling and Estimation

Justin Lazear

Jan 20, 2015

1 Introduction

Let us construct a very simple foreground as a toy example for use in our explorations. Since we are working only on simulated data and we are more interested in the general properties of our methods rather than the precise details of the results, a toy model is sufficient.

2 Thermal Dust Foreground

At high frequencies and large angular scales, dust dominates the foreground (Fig. 1) in intensity. With this in mind, we will begin by constructing a foreground map that comprises only dust.

Let us model the thermal dust emission as a power law,

$$I_\nu(p) = I_{\nu_0}(p)\left(\frac{\nu}{\nu_0}\right)^\beta \tag{1}$$

where I_ν is the spectral intensity in MJy/sr, I_{ν_0} is some reference amplitude map at the reference frequency ν_0, and β is the spectral index. So given a map $I_{\nu_0}(p)$ at frequency ν_0, we may construct a map of the thermal dust emission at an arbitrary frequency by scaling it by $\left(\frac{\nu}{\nu_0}\right)^\beta$. We ignore more sophisticated models that involve modeling the dust as particles at a particular temperature with a particular emissivity.

Let us use the Planck thermal dust component map[1] [8] at 353 GHz as our reference map (Fig. 2). We may then construct a thermal dust emission foreground map at an arbitrary frequency by scaling the reference map using Eq. (1) with $\nu_0 = 353\,\mathrm{GHz}$.

Some pixels in the Planck dust emission map have a negative intensity. These can potentially cause problems and are not physically realizable, so we replace the value of such pixels with 0.

[1] This map is produced by the Planck team by using a parameterized CMB + Foreground model and an MCMC solver to minimize the χ^2 of the model given the data, the `Commaner-Ruler` algorithm. The map generated by only one component of the model, using the optimal parameters, is the component map. In particular, we use only the intensity (I) component of the $N_{\mathrm{side}} = 256$ map.

The map is available from the Planck Legacy Archive under Maps → Foreground maps → Dust → `COM_CompMap_dust-commrul_0256_R1.00.fits`.

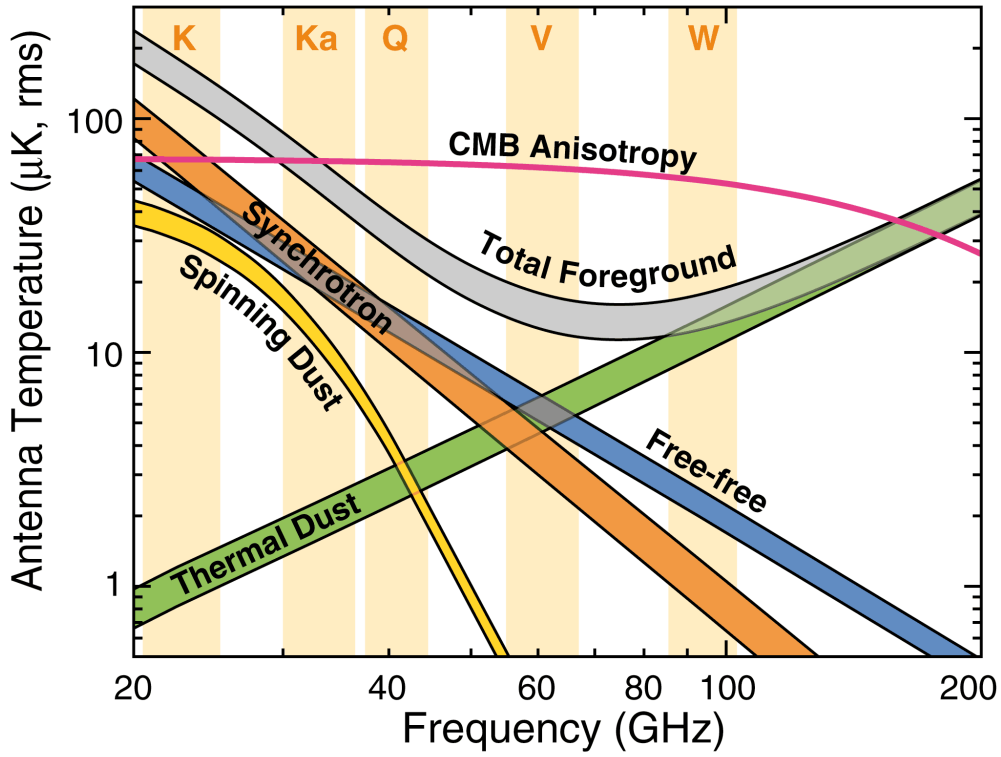

Figure 1: Frequency spectra of CMB temperature anisotropies and foregrounds. Above 80 GHz, the thermal dust is the dominant contributor. From Bennett et al 2009 [1].

We note that our power law is not in thermodynamic temperature units, but is rather in MJy/sr. This is incompatible with our sky maps, which are typically in thermodynamic temperature units (K). The conversion between spectral intensity I_ν and thermodynamic temperature T is

$$I_\nu = B_\nu(T) = \frac{2h\nu^3}{c^2}\frac{1}{\exp\left(h\nu/k_BT\right)-1} \tag{2}$$

$$T = B_\nu^{-1}(I_\nu) = \frac{h\nu}{k_B}\frac{1}{\log\left(1+\frac{2h\nu^3}{I_\nu c^2}\right)} \tag{3}$$

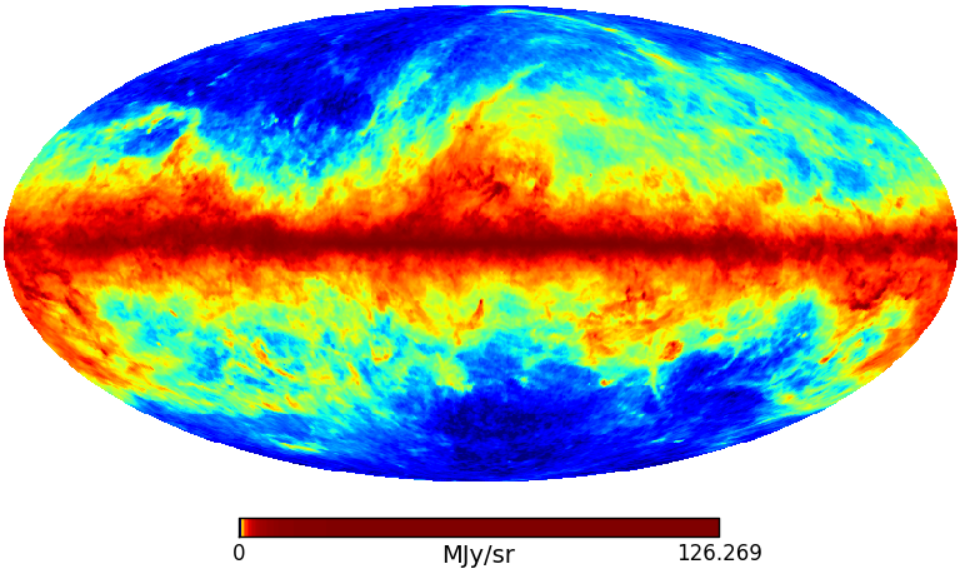

Figure 2: Planck thermal dust emission component map (from `Commander-Ruler` algorithm) at 353 GHz. From `COM_CompMap_dust-commrul_0256_R1.00.fits` intensity field. Histogram is equalized. Pixels that had a negative value in the original map have had their value replaced with 0.

so our power law (Eq. (1)) gives us the transformation

$$T = B_\nu^{-1}\left(I_{\nu_0}\left(\frac{\nu}{\nu_0}\right)^\beta\right)$$

$$T = \frac{h\nu}{k_B}\frac{1}{\log\left(1+\frac{2h\nu^{3-\beta}}{c^2\nu_0^{-\beta}}\frac{1}{I_{\nu_0}}\right)} \tag{4}$$

$$T = \frac{h\nu}{k_B}\frac{1}{\log\left[1+\left(\frac{\nu}{\nu_0}\right)^{3-\beta}\left(\exp\frac{h\nu_0}{k_BT_0}-1\right)\right]} \tag{5}$$

3 Polarized Dust Intensity

As a simple estimate of the polarized dust intensity, let us suppose that there is a constant polarization fraction of the thermal dust intensity,

$$p = \frac{I_p}{I} = \frac{\sqrt{Q^2+U^2+V^2}}{I} \tag{6}$$

where I_p is the polarized intensity, Q, U, and V are the polarized components of the Stokes vector, and I is the total intensity. Planck estimates that maximum polarization fraction is $p_{\max} = 20\%$[2], so we will use that as a pessimistic limit across the whole sky. In reality, we expect the polarization fraction to be smaller than this, especially in the galactic plane, where Planck reports the polarization fraction to typically be closer to 5%.

We may then construct a polarized intensity map

$$I_p(p) = p_{\max} I_\nu(p) \tag{7}$$

where p here is the pixel index and $p_{\max} = 20\%$ is the maximum polarization fraction. Note that this procedure should be done in spectral intensity units rather than thermodynamic temperature units, since the conversion is nonlinear, $B_\nu^{-1}(p_{\max} I_\nu) \neq p_{\max} B_\nu^{-1}(I_\nu)$.

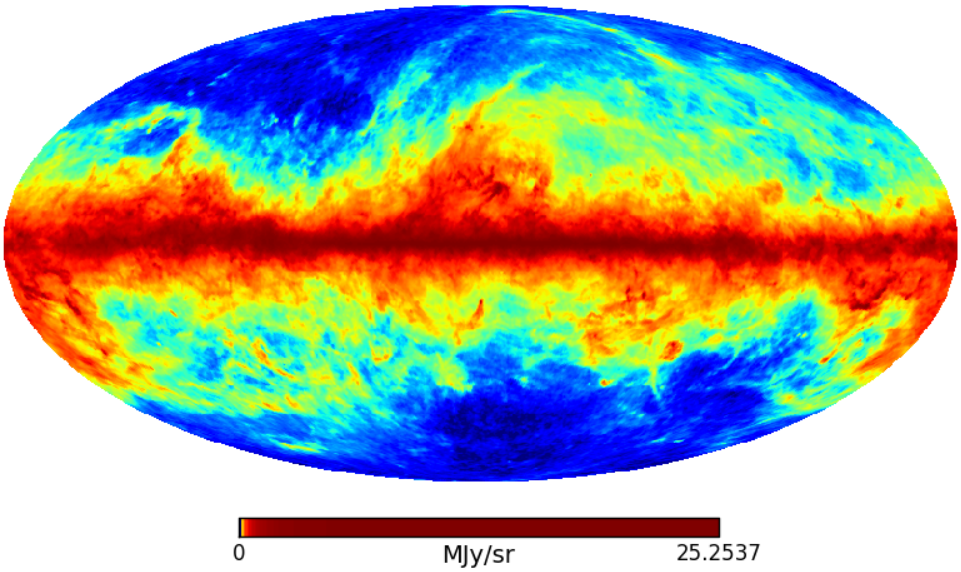

Figure 3: Naive polarized dust intensity $I_p = pI$. Uses a constant polarization fraction $p = p_{\max} = 0.2$ to construct a map from the thermal dust intensity map.

4 Polarized Dust Components

The polarized dust intensity map does not contain all of the information about the polarized radiation. We note from the definition of I_p,

$$I_p = \sqrt{Q^2 + U^2 + V^2} \tag{8}$$

that at each frequency and in each pixel, we must specify 3 numbers Q, U, and V (equivalently, the E-field vector components in some coordinate system, E_x and E_y, and the phase between the E-field components, $\phi \equiv \theta_x - \theta_y$)[4] to fully specify the polarized light.

4.1 Random Ensemble

Let us construct a very naive random ensemble of maps based on the information presented so far.

We assume that the circularly polarized component V is small[6], so we will set it to 0 and ignore it. This leaves us 2 numbers that we need to specify. Since we do not know the true values, we will randomly select a combination of Q and U that agrees with the polarized intensity map. Then an ensemble of such realizations will describe all possible Q and U maps that combine to construct the particular I_p map. If there is no physical phenomenon that would bias the true Q and U maps, then we can assume that our particular sky is one such realization of our ensemble and that the properties of the ensemble will estimate the properties of the true phenomena.

We must generate an unbiased ensemble by sampling Q and U in a symmetric way. We note that we have 2 unknowns (Q and U) and 1 constraint equation, so we must sample 1 random number to fully specify each realization. A simple uniform sampling of either Q or U does not uniformly sample the space of possible $\{Q, U\}$ values. Q and U describe a circle with radius I_p, so the space of possible choices of Q and U is a circle, which has only a single free parameter, the angle θ[2]. In radial coordinates,

$$Q + iU = I_p e^{i\theta}. \tag{9}$$

Since $|\mathrm{d}\theta|$ is invariant under reflection ($\theta \to -\theta$) and translation ($\theta \to \theta + \theta_0$), a uniform sampling of θ will uniformly sample the $\{Q, U\}$ space.

Let $\Theta \sim \mathcal{U}(0, 2\pi)$ be a uniformly distributed random variable over the range 0 to 2π. Then a number θ drawn from Θ can be used to construct Q and U from I_p for each pixel p,

$$\text{for } \theta(p) \in \Theta \sim \mathcal{U}(0, 2\pi), \qquad \begin{array}{l} Q(p) = I_p \cos\theta(p) = p_{\max} I_\nu \cos\theta(p) \\ U(p) = I_p \sin\theta(p) = p_{\max} I_\nu \sin\theta(p) \end{array} \tag{10}$$

for $p = 1, \ldots, N_{\mathrm{pix}}$. One such realization of Q and U maps is shown in Fig. 4.

It is clear that these maps have a nonsensical structure, with far too much variation on extremely small scales. Polarized dust in the interstellar medium relies on an interstellar magnetic field[5], so such small scale variations in dust polarization would imply significantly more structure on small scales than is consistent with current observations.

4.2 Synchrotron-tracking Polarization Direction Model

Both synchrotron[9] and dust[5] depend on the interstellar magnetic field in which their photons originate. If both phenomena produce radiation from the same region, then they are coupled to the same magnetic field, and hence we would expect some correlation between the synchrotron and dust components. In particularly, the synchrotron polarization angle should be a tracer of the dust polarization angle[3].

[2]Note that the angle θ does not directly correspond to the polarization angle, since the Stokes parameters are spin-2. The polarization angle γ is related to the sampling angle θ by $\theta = 2\gamma$.

To this end, we use the WMAP 23 GHz synchrotron component Q and U maps and estimate from them the polarization angle,

$$\gamma = \frac{1}{2}\arctan\left(-U, Q\right) \tag{11}$$

where we follow the convention of Delabrouille et al. for the orientation of the Stokes parameters. Following Delabrouille et al., we smooth the Q and U maps to 3° before computing the polarization angle map $\gamma(p)$. We note that the polarization angle map is independent of frequency.

These angle maps may then be applied to the polarization intensity maps of Section 3 to get the Q and U components of the polarized dust,

$$Q(p) = I_p(p)\cos 2\gamma(p) = p_{\max} I_\nu(p)\cos 2\gamma(p) \tag{12}$$
$$U(p) = I_p(p)\sin 2\gamma(p) = p_{\max} I_\nu(p)\sin 2\gamma(p). \tag{13}$$

The resulting polarization angle map $\gamma(p)$ and example Q and U dust foreground maps at 353 GHz are shown in Figure 5.

We note that this smoothing procedure suppresses power at angular scales smaller than 3°, corresponding to supressing power at $\ell \gtrsim 60$. A Planck analysis[7] of mid-latitude dust at 353 GHz suggests that there is still a significant amount of power on these scales. One possible method of incorporating this would be to simply extend the power spectrum of our dust maps using the power law scaling found by Planck,

$$D_\ell^{XX} = A^{XX}(\ell/80)^{\alpha_{XX}+2} \tag{14}$$

where $\alpha_{XX} = -2.42 \pm 0.02$, $X \in \{E, B\}$, and then reconstructing the map from the power spectra.

References

[1] C. L. Bennett, D. Larson, J. L. Weiland, N. Jarosik, G. Hinshaw, N. Odegard, K. M. Smith, R. S. Hill, B. Gold, M. Halpern, E. Komatsu, M. R. Nolta, L. Page, D. N. Spergel, E. Wollack, J. Dunkley, A. Kogut, M. Limon, S. S. Meyer, G. S. Tucker, and E. L. Wright. Nine-year wilkinson microwave anisotropy probe (WMAP) observations: Final maps and results. *The Astrophysical Journal Supplement Series*, 208:20, October 2013.

[2] Planck Collaboration, P. A. R. Ade, N. Aghanim, D. Alina, M. I. R. Alves, C. Armitage-Caplan, M. Arnaud, D. Arzoumanian, M. Ashdown, F. Atrio-Barandela, J. Aumont, C. Baccigalupi, A. J. Banday, R. B. Barreiro, E. Battaner, K. Benabed, A. Benoit-Lvy, J.-P. Bernard, M. Bersanelli, P. Bielewicz, J. J. Bock, J. R. Bond, J. Borrill, F. R. Bouchet, F. Boulanger, A. Bracco, C. Burigana, R. C. Butler, J.-F. Cardoso, A. Catalano, A. Chamballu, R.-R. Chary, H. C. Chiang, P. R. Christensen, S. Colombi, L. P. L. Colombo, C. Combet, F. Couchot, A. Coulais, B. P. Crill, A. Curto, F. Cuttaia, L. Danese, R. D. Davies, R. J. Davis, P. de Bernardis, E. M. de Gouveia Dal Pino, A. de Rosa, G. de Zotti, J. Delabrouille, F.-X. Dsert, C. Dickinson, J. M. Diego, S. Donzelli, O. Dor, M. Douspis, J. Dunkley, X. Dupac, T. A. Enlin, H. K. Eriksen, E. Falgarone, K. Ferrire, F. Finelli, O. Forni, M. Frailis, A. A. Fraisse, E. Franceschi, S. Galeotta, K. Ganga, T. Ghosh, M. Giard, Y. Giraud-Hraud, J. Gonzlez-Nuevo, K. M. Grski, A. Gregorio, A. Gruppuso, V. Guillet, F. K. Hansen, D. L. Harrison, G. Helou, C. Hernndez-Monteagudo, S. R.

Hildebrandt, E. Hivon, M. Hobson, W. A. Holmes, A. Hornstrup, K. M. Huffenberger, A. H. Jaffe, T. R. Jaffe, W. C. Jones, M. Juvela, E. Keihnen, R. Keskitalo, T. S. Kisner, R. Kneissl, J. Knoche, M. Kunz, H. Kurki-Suonio, G. Lagache, A. Lhteenmki, J.-M. Lamarre, A. Lasenby, C. R. Lawrence, J. P. Leahy, R. Leonardi, F. Levrier, M. Liguori, P. B. Lilje, M. Linden-Vrnle, M. Lpez-Caniego, P. M. Lubin, J. F. Macas-Prez, B. Maffei, A. M. Magalhes, D. Maino, N. Mandolesi, M. Maris, D. J. Marshall, P. G. Martin, E. Martnez-Gonzlez, S. Masi, S. Matarrese, P. Mazzotta, A. Melchiorri, L. Mendes, A. Mennella, M. Migliaccio, M.-A. Miville-Deschnes, A. Moneti, L. Montier, G. Morgante, D. Mortlock, D. Munshi, J. A. Murphy, P. Naselsky, F. Nati, P. Natoli, C. B. Netterfield, F. Noviello, D. Novikov, I. Novikov, C. A. Oxborrow, L. Pagano, F. Pajot, R. Paladini, D. Paoletti, F. Pasian, T. J. Pearson, O. Perdereau, L. Perotto, F. Perrotta, F. Piacentini, M. Piat, D. Pietrobon, S. Plaszczynski, F. Poidevin, E. Pointecouteau, G. Polenta, L. Popa, G. W. Pratt, S. Prunet, J.-L. Puget, J. P. Rachen, W. T. Reach, R. Rebolo, M. Reinecke, M. Remazeilles, C. Renault, S. Ricciardi, T. Riller, I. Ristorcelli, G. Rocha, C. Rosset, G. Roudier, J. A. Rubio-Martn, B. Rusholme, M. Sandri, G. Savini, D. Scott, L. D. Spencer, V. Stolyarov, R. Stompor, R. Sudiwala, D. Sutton, A.-S. Suur-Uski, J.-F. Sygnet, J. A. Tauber, L. Terenzi, L. Toffolatti, M. Tomasi, M. Tristram, M. Tucci, G. Umana, L. Valenziano, J. Valiviita, B. Van Tent, P. Vielva, F. Villa, L. A. Wade, B. D. Wandelt, A. Zacchei, and A. Zonca. Planck intermediate results. XIX. an overview of the polarized thermal emission from galactic dust. *arXiv:1405.0871 [astro-ph]*, May 2014. arXiv: 1405.0871.

[3] J. Delabrouille, M. Betoule, J.-B. Melin, M.-A. Miville-Deschnes, J. Gonzalez-Nuevo, M. Le Jeune, G. Castex, G. de Zotti, S. Basak, M. Ashdown, J. Aumont, C. Baccigalupi, A. J. Banday, J.-P. Bernard, F. R. Bouchet, D. L. Clements, A. da Silva, C. Dickinson, F. Dodu, K. Dolag, F. Elsner, L. Fauvet, G. Fa, G. Giardino, S. Leach, J. Lesgourgues, M. Liguori, J. F. Macas-Prez, M. Massardi, S. Matarrese, P. Mazzotta, L. Montier, S. Mottet, R. Paladini, B. Partridge, R. Piffaretti, G. Prezeau, S. Prunet, S. Ricciardi, M. Roman, B. Schaefer, and L. Toffolatti. The pre-launch planck sky model: a model of sky emission at submillimetre to centimetre wavelengths. *Astronomy and Astrophysics*, 553:A96, May 2013.

[4] Marc Kamionkowski, Arthur Kosowsky, and Albert Stebbins. Statistics of cosmic microwave background polarization. *Phys. Rev. D*, 55(12):7368–7388, June 1997.

[5] A. Lazarian. Tracing magnetic fields with aligned grains. *Journal of Quantitative Spectroscopy and Radiative Transfer*, 106:225–256, July 2007.

[6] R. Mainini, D. Minelli, M. Gervasi, G. Boella, G. Sironi, A. Ba, S. Banfi, A. Passerini, A. De Lucia, and F. Cavaliere. An improved upper limit to the CMB circular polarization at large angular scales. *Journal of Cosmology and Astro-Particle Physics*, 08:033, August 2013.

[7] Planck Collaboration, R. Adam, P. A. R. Ade, N. Aghanim, M. Arnaud, J. Aumont, C. Baccigalupi, A. J. Banday, R. B. Barreiro, J. G. Bartlett, N. Bartolo, E. Battaner, K. Benabed, A. Benoit-Lvy, J.-P. Bernard, M. Bersanelli, P. Bielewicz, A. Bonaldi, L. Bonavera, J. R. Bond, J. Borrill, F. R. Bouchet, F. Boulanger, A. Bracco, M. Bucher, C. Burigana, R. C. Butler, E. Calabrese, J.-F. Cardoso, A. Catalano, A. Challinor, A. Chamballu, R.-R. Chary, H. C. Chiang, P. R. Christensen, D. L. Clements, S. Colombi, L. P. L. Colombo, C. Combet, F. Couchot, A. Coulais, B. P. Crill, A. Curto, F. Cuttaia, L. Danese, R. D. Davies, R. J. Davis, P. de Bernardis, G. de Zotti, J. Delabrouille, J.-M. Delouis, F.-X. Dsert, C. Dickinson, J. M. Diego, K. Dolag, H. Dole, S. Donzelli, O. Dor, M. Douspis, A. Ducout, J. Dunkley, X. Dupac, G. Efstathiou, F. Elsner, T. A. Enlin, H. K. Eriksen, E. Falgarone, F. Finelli, O. Forni, M. Frailis, A. A. Fraisse, E. Franceschi, A. Frejsel, S. Galeotta, S. Galli, K. Ganga, T. Ghosh, M. Giard, Y. Giraud-Hraud, E. Gjerlw, J. Gonzlez-Nuevo, K. M. Grski, S. Gratton, A. Gregorio, A. Gruppuso, V. Guillet, F. K. Hansen, D. Hanson, D. L. Harrison, G. Helou, S. Henrot-Versill, C. Hernndez-Monteagudo, D. Herranz, E. Hivon, M. Hobson, W. A. Holmes, K. M. Huffenberger, G. Hurier, A. H. Jaffe, T. R. Jaffe, J. Jewell, W. C. Jones, M. Juvela, E. Keihnen, R. Keskitalo, T. S. Kisner, R. Kneissl, J. Knoche, L. Knox, N. Krachmalnicoff, M. Kunz, H. Kurki-Suonio, G. Lagache, J.-M. Lamarre, A. Lasenby, M. Lattanzi, C. R. Lawrence, J. P. Leahy, R. Leonardi, J. Lesgourgues, F. Levrier, M. Liguori, P. B. Lilje,

M. Linden-Vrnle, M. Lpez-Caniego, P. M. Lubin, J. F. Macas-Prez, B. Maffei, D. Maino, N. Mandolesi, A. Mangilli, M. Maris, P. G. Martin, E. Martnez-Gonzlez, S. Masi, S. Matarrese, P. Mazzotta, A. Melchiorri, L. Mendes, A. Mennella, M. Migliaccio, S. Mitra, M.-A. Miville-Deschnes, A. Moneti, L. Montier, G. Morgante, D. Mortlock, A. Moss, D. Munshi, J. A. Murphy, P. Naselsky, F. Nati, P. Natoli, C. B. Netterfield, H. U. Nrgaard-Nielsen, F. Noviello, D. Novikov, I. Novikov, L. Pagano, F. Pajot, R. Paladini, D. Paoletti, B. Partridge, F. Pasian, G. Patanchon, T. J. Pearson, O. Perdereau, L. Perotto, F. Perrotta, V. Pettorino, F. Piacentini, M. Piat, E. Pierpaoli, D. Pietrobon, S. Plaszczynski, E. Pointecouteau, G. Polenta, N. Ponthieu, L. Popa, G. W. Pratt, S. Prunet, J.-L. Puget, J. P. Rachen, W. T. Reach, R. Rebolo, M. Remazeilles, C. Renault, A. Renzi, S. Ricciardi, I. Ristorcelli, G. Rocha, C. Rosset, M. Rossetti, G. Roudier, B. Rouill d'Orfeuil, J. A. Rubio-Martn, B. Rusholme, M. Sandri, D. Santos, M. Savelainen, G. Savini, D. Scott, J. D. Soler, L. D. Spencer, V. Stolyarov, R. Stompor, R. Sudiwala, R. Sunyaev, D. Sutton, A.-S. Suur-Uski, J.-F. Sygnet, J. A. Tauber, L. Terenzi, L. Toffolatti, M. Tomasi, M. Tristram, M. Tucci, J. Tuovinen, L. Valenziano, J. Valiviita, B. Van Tent, L. Vibert, P. Vielva, F. Villa, L. A. Wade, B. D. Wandelt, R. Watson, I. K. Wehus, M. White, S. D. M. White, D. Yvon, A. Zacchei, and A. Zonca. Planck intermediate results. XXX. the angular power spectrum of polarized dust emission at intermediate and high galactic latitudes. *ArXiv e-prints*, 1409:5738, September 2014.

[8] Planck Collaboration, P. A. R. Ade, N. Aghanim, C. Armitage-Caplan, M. Arnaud, M. Ashdown, F. Atrio-Barandela, J. Aumont, C. Baccigalupi, A. J. Banday, R. B. Barreiro, J. G. Bartlett, E. Battaner, K. Benabed, A. Benot, A. Benoit-Lvy, J.-P. Bernard, M. Bersanelli, P. Bielewicz, J. Bobin, J. J. Bock, A. Bonaldi, L. Bonavera, J. R. Bond, J. Borrill, F. R. Bouchet, F. Boulanger, M. Bridges, M. Bucher, C. Burigana, R. C. Butler, J.-F. Cardoso, G. Castex, A. Catalano, A. Challinor, A. Chamballu, R.-R. Chary, X. Chen, H. C. Chiang, L.-Y. Chiang, P. R. Christensen, S. Church, D. L. Clements, S. Colombi, L. P. L. Colombo, F. Couchot, A. Coulais, B. P. Crill, M. Cruz, A. Curto, F. Cuttaia, L. Danese, R. D. Davies, R. J. Davis, P. de Bernardis, A. de Rosa, G. de Zotti, J. Delabrouille, J.-M. Delouis, F.-X. Dsert, C. Dickinson, J. M. Diego, G. Dobler, H. Dole, S. Donzelli, O. Dor, M. Douspis, J. Dunkley, X. Dupac, G. Efstathiou, T. A. Enlin, H. K. Eriksen, E. Falgarone, F. Finelli, O. Forni, M. Frailis, A. A. Fraisse, E. Franceschi, S. Galeotta, K. Ganga, M. Giard, G. Giardino, Y. Giraud-Hraud, J. Gonzlez-Nuevo, K. M. Grski, S. Gratton, A. Gregorio, A. Gruppuso, F. K. Hansen, D. Hanson, D. L. Harrison, G. Helou, S. Henrot-Versill, C. Hernndez-Monteagudo, D. Herranz, S. R. Hildebrandt, E. Hivon, M. Hobson, W. A. Holmes, A. Hornstrup, W. Hovest, G. Huey, K. M. Huffenberger, A. H. Jaffe, T. R. Jaffe, J. Jewell, W. C. Jones, M. Juvela, E. Keihnen, R. Keskitalo, T. S. Kisner, R. Kneissl, J. Knoche, L. Knox, M. Kunz, H. Kurki-Suonio, G. Lagache, A. Lhteenmki, J.-M. Lamarre, A. Lasenby, R. J. Laureijs, C. R. Lawrence, M. Le Jeune, S. Leach, J. P. Leahy, R. Leonardi, J. Lesgourgues, M. Liguori, P. B. Lilje, M. Linden-Vrnle, M. Lpez-Caniego, P. M. Lubin, J. F. Macas-Prez, B. Maffei, D. Maino, N. Mandolesi, A. Marcos-Caballero, M. Maris, D. J. Marshall, P. G. Martin, E. Martnez-Gonzlez, S. Masi, M. Massardi, S. Matarrese, F. Matthai, P. Mazzotta, P. R. Meinhold, A. Melchiorri, L. Mendes, A. Mennella, M. Migliaccio, K. Mikkelsen, S. Mitra, M.-A. Miville-Deschnes, D. Molinari, A. Moneti, L. Montier, G. Morgante, D. Mortlock, A. Moss, D. Munshi, J. A. Murphy, P. Naselsky, F. Nati, P. Natoli, C. B. Netterfield, H. U. Nrgaard-Nielsen, F. Noviello, D. Novikov, I. Novikov, I. J. O'Dwyer, S. Osborne, C. A. Oxborrow, F. Paci, L. Pagano, F. Pajot, R. Paladini, D. Paoletti, B. Partridge, F. Pasian, G. Patanchon, T. J. Pearson, O. Perdereau, L. Perotto, F. Perrotta, V. Pettorino, F. Piacentini, M. Piat, E. Pierpaoli, D. Pietrobon, S. Plaszczynski, P. Platania, E. Pointecouteau, G. Polenta, N. Ponthieu, L. Popa, T. Poutanen, G. W. Pratt, G. Przeau, S. Prunet, J.-L. Puget, J. P. Rachen, W. T. Reach, R. Rebolo, M. Reinecke, M. Remazeilles, C. Renault, A. Renzi, S. Ricciardi, T. Riller, I. Ristorcelli, G. Rocha, M. Roman, C. Rosset, G. Roudier, M. Rowan-Robinson, J. A. Rubio-Martn, B. Rusholme, E. Salerno, M. Sandri, D. Santos, G. Savini, F. Schiavon, D. Scott, M. D. Seiffert, E. P. S. Shellard, L. D. Spencer, J.-L. Starck, R. Stompor, R. Sudiwala, R. Sunyaev, F. Sureau, D. Sutton, A.-S. Suur-Uski, J.-F. Sygnet, J. A. Tauber, D. Tavagnacco, L. Terenzi, L. Toffolatti, M. Tomasi, M. Tristram, M. Tucci, J. Tuovinen, M. Trler, G. Umana, L. Valenziano, J. Valiviita, B. Van Tent, J. Varis, M. Viel, P. Vielva, F. Villa, N. Vittorio, L. A. Wade, B. D. Wandelt, I. K. Wehus, A. Wilkinson, J.-Q. Xia, D. Yvon, A. Zacchei,

and A. Zonca. Planck 2013 results. XII. diffuse component separation. *Astronomy and Astrophysics*, 571:A12, November 2014.

[9] George B. Rybicki and Alan P. Lightman. *Radiative Processes in Astrophysics*. Wiley-VCH, Weinheim, March 1985.

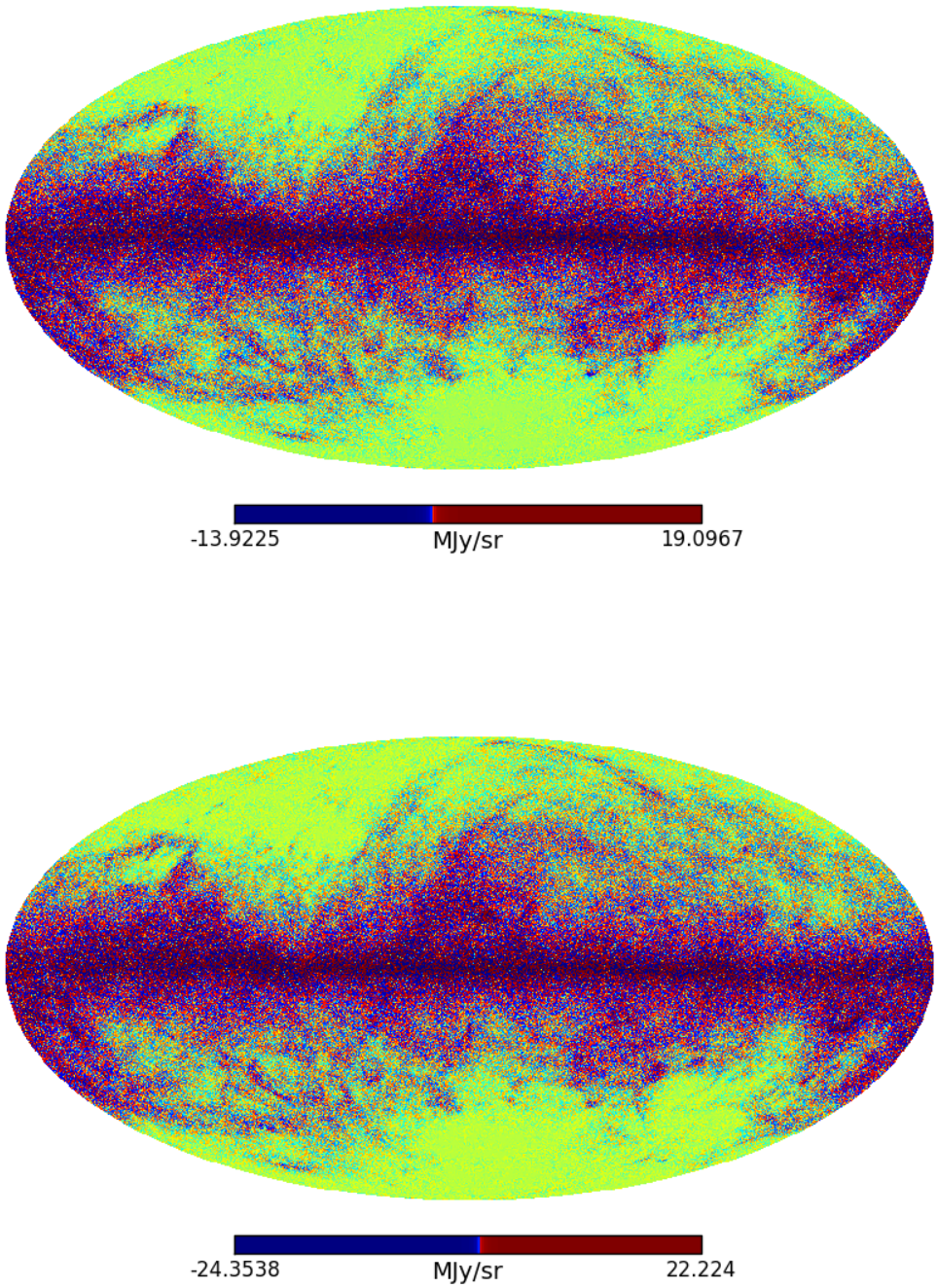

Figure 4: *Top*: One realization of a Q map in which each pixel has an independent angle θ that is uniformly sampled from 0 to 2π, and $Q(p) = I_p \cos\theta(p)$. *Bottom*: A U map that matches the above Q map.

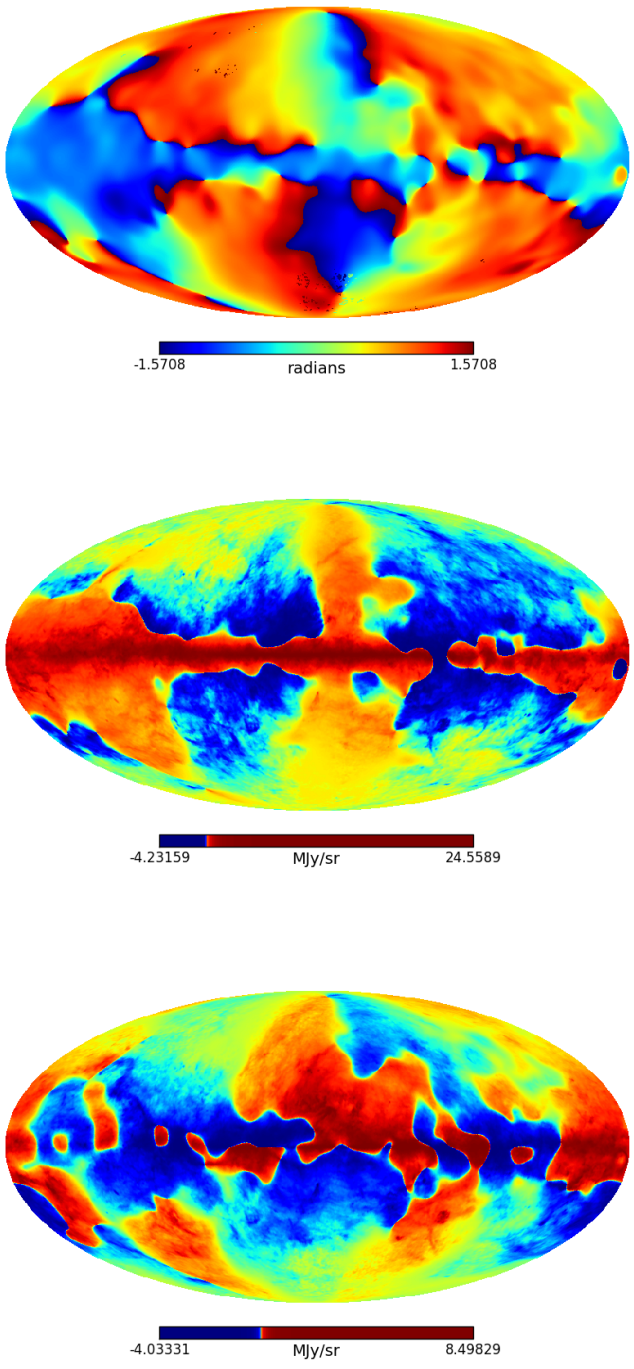

Figure 5: *Top*: The polarization angle map $\gamma(p)$. The map is smoothed to 3°. *Middle*: The resulting polarized dust foreground Q map at 353 GHz. *Bottom*: The resulting polarized dust foreground U map at 353 GHz.